Interaction of *Mycoplasma synoviae* with chicken synovial sheath cells contributes to macrophage recruitment and inflammation

Bin Xu,[*,†] Rui Liu,[*,†] Meijuan Ding,[*,†] Jingfeng Zhang,[*,†] Huawei Sun,[*,†] Chuanmin Liu,[*,†] Fengying Lu,[*,†] Sha Zhao,[*,†] Qunxing Pan,[*,†] and Xiaofei Zhang[*,†,1]

[*]*Key Laboratory of Veterinary Biological Engineering and Technology of Ministry of Agriculture, Institute of Veterinary Medicine, Jiangsu Academy of Agricultural Sciences, Nanjing, China; and* [†]*National Center for Engineering Research of Veterinary Bio-Products, Jiangsu Academy of Agricultural Sciences, Nanjing, China*

ABSTRACT *Mycoplasma synoviae* (**MS**) is an important avian pathogen causing considerable economic hardship in the poultry industry. A major inflammation caused by MS is synovitis that occurs in the synovial tendon sheath and joint synovium. However, the overall appearance of pathological changes in the tendon sheath and surrounding tissues caused by MS infection at the level of pathological tissue sections was poor. Studies on the role of MS and synovial sheath cells (**SSCs**) interaction in the development of synovitis have not been carried out. Through histopathological observation, our study found that a major MS-induced pathological change of the tendon sheath synovium was extensive scattered and focal inflammatory cell infiltration of the tendon sheath synovial layer. *In vitro* research experiments revealed that the CFU numbers of MS adherent and invading SSC, the levels of expression of various pattern recognition receptors, inflammatory cytokines, and chemokines coding genes, such as IL-1β, IL-6, IL-8, CCL-20, RANTES, MIP-1β, TLR7, and TLR15 in SSCs, and chemotaxis of macrophages were significantly increased when the multiplicity of infection (**MOI**) of MS to SSC were increased tenfold. The expression level of IL-12p40 in SSC was significantly higher when the MOIs of MS to SSC were increased by a factor of 100. The interaction between MS and SSC can activate macrophages, which was manifested by a significant increase in the expression of IL-1β, IL-6, IL-8, CCL-20, RANTES, MIP-1β, and CXCL-13. This study systematically demonstrated that the interaction of MS with chicken SSC contributes to the inflammatory response caused by the robust expression of related cytokines and macrophage chemotaxis. These findings are helpful in elucidating the molecular mechanism of MS-induced synovitis in chickens.

Key words: *Mycoplasma synoviae*, synovial sheath cell, macrophage, synovitis, chemotaxis

2020 Poultry Science 99:5366–5377
https://doi.org/10.1016/j.psj.2020.08.003

INTRODUCTION

Mycoplasma synoviae (**MS**) is a major avian pathogen. Its infection can cause subclinical to acute and chronic respiratory damage, synovitis, osteoarthritis, and other diseases in chickens, turkeys, and other poultry worldwide. Although these infections rarely cause direct death of poultry, they lead to obvious lameness, growth retardation, ketone body degradation, higher morbidity and mortality to other pathogens, lower egg production rate, and an increase in the probability of producing eggs with eggshell apex abnormalities, causing a serious harm to poultry farming (Dufour-Gesbert et al., 2006; Oh et al., 2010; Kursa et al., 2019). From 2010 to 2015, Sun et al. detected the prevalence of MS in 9,773 broiler flocks in 16 provinces of China, revealing that the average infection rate of MS in eggs was 16.29% (Sun et al., 2017). Xue et al. (2017) used ELISA to detect 44,395 sera from unvaccinated chickens from 21 provinces of China from 2010 to 2015, showing the overall positive rate of MS was 41.19%. However, despite the clinical relevance of MS, investigations on the pathogenesis leading to synovitis are limited.

Until now, the study of synovitis in chickens caused by MS has been limited to the observation of clinical symptoms and pathological changes (Walker et al., 1978; Lockaby et al., 1998; Sun et al., 2017). MS-infected chickens show lesions of the wing joints, intertarsal

Received November 20, 2019.
Accepted August 15, 2020.

[1]Corresponding author: xiaofei0804@sina.com

joints, digital flexor tendons, metatarsal extensor tendons, and footpads, manifested as the viscous to caseous exudation, tissue hyperplasia and hypertrophy, and the infiltration of inflammatory cells. MS can be isolated or identified from diseased synovial tissues by medium culture or PCR testing (Lockaby et al., 1998). Nevertheless, the overall appearance of the tendon, tendon sheath, and surrounding tissues at the level of pathological tissue sections after MS infection was poor. In addition, the molecular mechanisms underlying the development of synovitis in tendon sheaths are not known.

Tendon sheaths are classified as extrinsic tissues in contrast to tendon fibers and epitenons, which are intrinsic structures (Kannus, 2000). The surrounding structures of the tendons can be divided into 5 categories. One of them is the synovial sheath, which only covers tendon fibers in high-friction areas, such as the flexor and extensor tendons (Greenlee et al., 1975; Kannus, 2000). Similar to the joint, the inner surface of the synovial tendon sheath is covered with cell-rich layers, which consist of 2 kinds of cells, macrophage-like cells and fibroblast-like cells. Macrophage-like cells accumulated in the mesotendon, but few in other regions. Fibroblast-like cells, the main cell type that constitutes the tendon sheath tissue, are distributed in the entire length of the synovial layer in the tendon sheath (Kohama et al., 2002).

The interactions between mycoplasma, such as *Mycoplasma genitalium* and *Mycoplasma gallisepticum* (**MG**), and corresponding major infected epithelial cells play an important role in the initial stages of various inflammation processes, including activation of pattern recognition receptors, secretion of inflammatory cytokines and chemokines, and the recruitment and activation of immune cells (McGowin et al., 2009a, 2009b; Majumder et al., 2014; Majumder and Silbart, 2016). MS or its membrane protein has been reported to significantly stimulate macrophages to upregulate the expression of IL-1β, IL-6, and TLR15, as well as significantly stimulate chondrocytes to upregulate the expression of TLR15 (Lavric et al., 2007; Oven et al., 2013). Whether the interaction between MS and fibroblast-like synovial sheath cells (**SSCs**) plays similar roles remains to be determined and will be the subject of this present study.

MATERIALS AND METHODS

Ethics Statements

All animal experiments were performed in Jiangsu Academy of Agricultural Sciences (**JAAS**) with the approval of the Committee on the Ethics of Animal Experiments of JAAS (JAAS no. 20141107). All experimental procedures conformed to the guidelines of Jiangsu Province Animal Regulations (Government Decree No. 45) in accordance with international law.

MS Culture Conditions

The MS virulent strain HN01 was isolated by us from a sick chicken with synovitis in the Henan province, China, and maintained in our laboratory. MS was cultured in modified Frey's broth or solid medium at 37°C with 5% CO_2 as described previously (Walker et al., 1978; Dusanic et al., 2009). The strain used in this study was passed fewer than 5 times *in vitro*.

Experimental Infection

Xueshan native chicken eggs were purchased from Jiangsu Lihua Animal Husbandry Co., Ltd. (Changzhou, China) and placed in an automatic incubator (model ZF528; Zhengda Incubation Equipment Factory, Dezhou, China) at 37.8°C for 21 d. New-born chicks were housed and reared until the age of 25 wk in barrier isolation units with high-efficiency particulate air-filtered air under negative pressure (model QXI-2; Qiangxing Equipment Technology Co., Ltd., Qingdao, China). Every 2 wk, chickens in different barrier isolation units were randomly reassigned. Chickens were tested negative for the avian influenza virus, Newcastle disease virus, infectious bronchitis virus, MS, and MG. Then, 20 female chickens were divided randomly into 2 groups, which were housed and reared in 2 sets of independent barrier isolation units. Each chicken in one group (n = 10) was challenged with 0.1 mL of 1.0×10^8 CFU/mL phosphate-buffered saline (**PBS**, pH 7.4) containing MS by footpad injection. Each chicken in the other group (n = 10) was challenged with 0.1 mL of PBS (pH 7.4) by footpad injection. After 10 d of incubation, the chickens were euthanized by exsanguination under deep nembutal anesthesia (45 μg/g of body weight, intraperitoneal injection; Shanghai Chemical Factory, Shanghai, China) and for necropsy. The metatarsal extensor tendons with synovial sheaths were collected, fixed immediately in 4% paraformaldehyde, decalcified in 20% EDTA, processed for paraffin embedding, sectioned at 4-μm thicknesses, and stained with hematoxylin and eosin following standard histological protocols. Pathological tissue sections were scanned using Pannoramic 250 Flash III (3DHISTECH, Budapest, Hungary). CaseViewer software v2.0.2 (3DHISTECH, Budapest, Hungary) was used for observation of scanned parts of pathological tissue sections.

Primary Chicken SSC and HD-11 Cells Culture

Primary chicken SSCs were harvested as previously described (Ozturk et al., 2008). Briefly, the synovial layer sheath of metatarsal extensor tendon was harvested under sterile conditions. Tissues were rinsed with 0.1 mol sterile PBS (pH 7.2), cut into small pieces of 1 mm^3, and digested with 0.1% trypsin in PBS for 30 min. Then the mixture was centrifuged. The pellets were washed with PBS and digested in 0.1% collagenase in Dulbecco's modified Eagle medium (**DMEM**, 11965-092; GIBCO, Waltham, MA) containing 10% fetal bovine serum (**FBS**, 10099-141; GIBCO, Waltham, MA), 100 U/mL penicillin, and 100 mg/mL streptomycin for 2 h at 37°C. After the digestion process, cells

were filtered through a 70-μm nylon sterile filter, washed twice with DMEM, and cultured in DMEM with 10% FBS at 37°C with 5% CO_2. The third-to-sixth generation cells were used for experimental research. The chicken HD-11 macrophage cell line was kindly provided by Professor Hongjie Fan at the College of Veterinary Medicine, Nanjing Agricultural University. HD11 cells were cultured in DMEM with 10% FBS at 37°C with 5% CO_2.

Adherence and Invasion Assays

These 2 assays were performed as reported previously with some modifications (Dusanic et al., 2009; Yu et al., 2018). The SSCs were cultured to approximately 5.0×10^5 cells/well in 24-well plates and used in the assays. MS in the logarithmic growth phase was harvested by centrifugation (5,000 × *g*, 5 min), washed with DMEM, and added to SSCs at a multiplicity of infection (**MOI**) of 0.1, 1, or 10, respectively. After 6 h of incubation at 37°C under 5% CO_2, the cells were washed with sterile PBS. For the adherence assays, SSCs were added to double-distilled water to lyse the cells, and cell-associated MS were recovered. For the invasion assays, DMEM containing 500 μg/mL gentamicin (Sigma) was added to SSC and incubated for an additional hour to kill extracellular MS. Then, after another 3 washes with PBS, the cells were lysed with double-distilled water to recover intracellular MS. Recovered MS were calculated using the plate count method. The assays were performed as 3 independent experiments.

Extraction of Total Cellular RNA, RT-PCR, and qPCR Assays

The SSCs, cultured to approximately 5.0×10^5 cells/well in 24-well plates, were incubated with HN01 at an MOI of 0.1, 1, or 10 for 12 h or at an MOI of 10 for 6, 12, and 24 h. Then the SSCs were used for total RNA extraction.

The coculture (Supplementary Table 1) studies of MS, SSC, and HD11 cells were performed as reported before with some modifications (Majumder and Silbart, 2016). HD11 cells were plated at a concentration of approximately 10^4 cells/well in 0.4-μm-pore-size Transwells (3413; Corning, New York) for 18 h before the coculture assay. The SSCs, cultured to approximately 5.0×10^5 cells/well in 24-well plates, were incubated with or without HN01 at an MOI of 10 for 2 h. The SSCs were washed 5 times with PBS to remove the unattached MS, supplemented with DMEN containing 2% FBS, and cultured for 6 h. Transwells containing HD11 cells were plated over each well. The coculture was maintained for 6 h. The HD11 cells were used for total RNA extraction. The supernatants were transferred to the modified Frey's broth for 7 d to observe the growth of mycoplasma and were used to detect the antigenic components of MS by ELISA using rabbit polyclonal antibodies against MS.

The total RNA of SSCs or HD11 cells was extracted using the RNAiso Plus procedure (9108; TaKaRa, Kusatsu, Japan) according to the handbook. cDNA Synthesis was performed using the PrimeScript RT reagent kit (RR037A; TaKaRa, Kusatsu, Japan). mRNA Levels were measured with the SYBR Premix Ex Taq kit (RR42LR; TaKaRa, Kusatsu, Japan) according to the manufacturer's instructions. The primers used in these experiments are listed in Table 1. The GAPDH gene was amplified as a reference (Majumder and Silbart, 2016). Relative changes in gene transcription were calculated using the comparative C_T method (Livak and Schmittgen, 2001). Each set of qPCR assay was performed 3 times with independent biological replicates.

Surface markers of SSC and HD11 cells were identified by RT-PCR analysis. The primers used in this experiment are listed in Table 2.

Chemotaxis

The chemotaxis assay was performed as reported before (Majumder and Silbart, 2016) with some modifications. Briefly, after infecting the SSCs in the cell plate for 2 h with MS at an MOI of 0.1, 1, or 10, the MS that had not adhered to the surface of the SSC were washed away with PBS, and the cells were incubated for 6 h. Then 50 μL of the MS-free supernatants was transferred into a new cell plate well containing fresh DMEM. The detection of mycoplasma components was the same as that described previously. DMEM containing 100 ng/mL chicken MIP-1β (ICT-6396; Kingfisher Biotech, St. Paul, MN) was used as a positive control. The supernatant from the uninfected SSCs served as a negative control. Transwells of 5.0-μm pore size (3421, Corning, New York) containing 1.0×10^6 HD11 cells in the upper chamber were placed in the wells of the cell plate and cultured for another 4 h. After incubation, the HD11 cells on the bottom side of Transwell were stained using a Fisher HealthCare PROTOCOL Hema 3 Stat Pack (23-123869; Fisher Scientific, Sunnyvale, CA) according to the manufacturer's procedure. The membrane then was air-dried, and cells were counted under a light microscope at 10× magnification. The number of macrophages that migrate to the bottom of Transwell was used to determine the strength of chemotaxis to macrophages. Three independent experiments were performed.

Statistical Analysis

Data were analyzed using GraphPad Prism version 7.0 (GraphPad Software, https://www.graphpad.com/). Data were collected from 3 independent experiments of assays mentioned previously and presented as the means with standard errors. Statistical analyses for all pairwise comparisons were assessed using unpaired *t* test. Differences were considered to be significant for $P < 0.05$.

Table 1. Primers used for qPCR analysis.

Target gene	Oligonucleotide sequence (5'→3')	GenBank accession no. of target gene	Source or reference of primer sequences
TLR1	F: AGCTGTGTCAGCATGAGAGGAACT R: AGTTGGGTGACAACACAAAGATGG	NM_001007488.4	Oven et al., 2013
TLR2	F: AGAACGACTCCAACTGGGTGGAAA R: AGAGCGTCTTGTGGCTCTTCTCAA	NM_001161650.1	Oven et al., 2013
TLR4	F: TTTTGCCAACCTGACCTCT R: CAGCCTGTTTGTTTCCCTC	NM_001030693.1	This study
TLR5	F: ACTCCCTTCCTTCCCACA R: AAGAACATACAGGTCACCCAG	NM_001024586.1	This study
TLR7	F: TTGCTGACCTAAGGGTGTTC R: AGTGCCTGCTGTATTGCTCT	NM_001011688.2	This study
TLR15	F: AACCTGGTGCATTTGAGAACCTGC R: TTTCAGGTGAGGTGCAAGACCAGA	NM_001037835.1	Oven et al., 2013
IL-1β	F: GCTGGAACTGGGCAGAT R: GGTAGAAGATGAAGCGGGTC	NM_204524.1	Majumder et al., 2014
IL-6	F: CCTGTTCGCCTTTCAGACCTA R: AGTCTGGGATGACCACTTC	NM_204628.1	Majumder et al., 2014
IL-8	F: GTGCATTAGCACTCATTCTAAGTT R: GGCCATAAGTGCCTTTACG	NM_205498.1	Majumder et al., 2014
CCL-20	F: GCCAGAAGCTCAAGAGGATG R: TCCAGAAGTTCAACGGTTCC	NM_204438.2	Majumder et al., 2014
CXCL-13	F: GGACCTCCCGAAGCTGAA R: TCTGCCTTTCCACGGATACAT	NM_001348656.1	Majumder and Silbart, 2016
RANTES	F: TATTTCTACACCAGCAGCAAATG R: GCAGACACCTCAGGTCC	AY037859.1	Majumder and Silbart, 2016
MIP-1β	F: CTGCTTCACCTACATCTCCC R: GTCCTGTACCCAGTCGTT	NM_001030360.2	Majumder and Silbart, 2016
IL-12p40	F: TGAAGGAGTTCCCAGATGC R: CGTCTTGCTTGGCTCTTTATA	AY262752.1	Majumder and Silbart, 2016
IFN-γ	F: TAGCTGACGGTGGACCTA R: CTCAGATATGTGTTTGATGTGCG	NM_205149.1	Majumder and Silbart, 2016
GAPDH	F: ATTCTACACACGGACACTTCA R: CACCAGTGGACTCCACAACATA	NM_204305.1	Majumder and Silbart, 2016

Abbreviations: F, forward primer; R, reverse primer.

RESULTS

Pathological Tissue Section Observation of the Lesional Tendon Sheath

The skin tissue and tendon sheath that covered the surface of the metatarsal extensor tendon of normal chicken were slack. The subcutaneous tissue covering the tendon sheath of the metatarsal extensor tendon consisted of dense connective tissue (Figure 1A). The edge of the dense connective tissue, which faced the tendon sheath, contained several layers of fibrous cells with blood vessels that passed through the area (Figure 1A). The normal tendon sheath synovium consisted of several layers of loose fibrous cell layers (the synovial cell layer) and multilayered closely packed fibrous sheath, as reported in other articles on synovial sheath structures (Figures 1C, 1E) (Greenlee et al., 1975; Kannus, 2000). The epitenon covering the surface of the tendon had 2-3 layers of fibrous cells, through which the blood vessels of a single layer of cells passed (Figures 1C, 1E). Almost no leukocytes were seen in these tissues mentioned previously (Figures 1A, 1C, 1E).

After the chickens were infected with MS, the metatarsal extensor tendon position of 80% of the challenged chickens showed different degrees of skin tightening and swelling under the skin. Some were bilateral swelling, and some only showed obvious swelling in one leg. After incision, there was viscous exudate in the tendon sheath cavity. Diseased metatarsal extensor tendon sheath from 6 challenged chickens was isolated. MS was isolated from diseased sheath tissues, which were obtained from 5 challenged chickens by medium culture. Under pathological tissue section observation, the dense connective tissue under the skin and the fibrous cells layer at the edge of the dense connective tissue showed vascular hyperplasia and perivascular focal leukocyte infiltration (Figures 1B, 1D). The layer of fibrous cells at the edge of the dense

Table 2. Primers used for RT-PCR analysis.

Target gene	Oligonucleotide sequence (5'→3')	GenBank accession no. of target gene	Source or reference of primer sequences
Cadherin-11	F: GAAGGACAAGTTTTGCATCG R: GTTCGGATAATTCCTGTTTGAG	NM_001004371.1	This study
CD45	F: ACTCGGCTGAAGTTACGCT R: GTTACATTTCTGGCAGTAGGAT	NM_204417.2	This study
GAPDH	F: AAAGTCGGAGTCAACGGAT R: GACGCTGGGATGATGTTCT	NM_204305.1	This study

Abbreviations: F, forward primer; R, reverse primer.

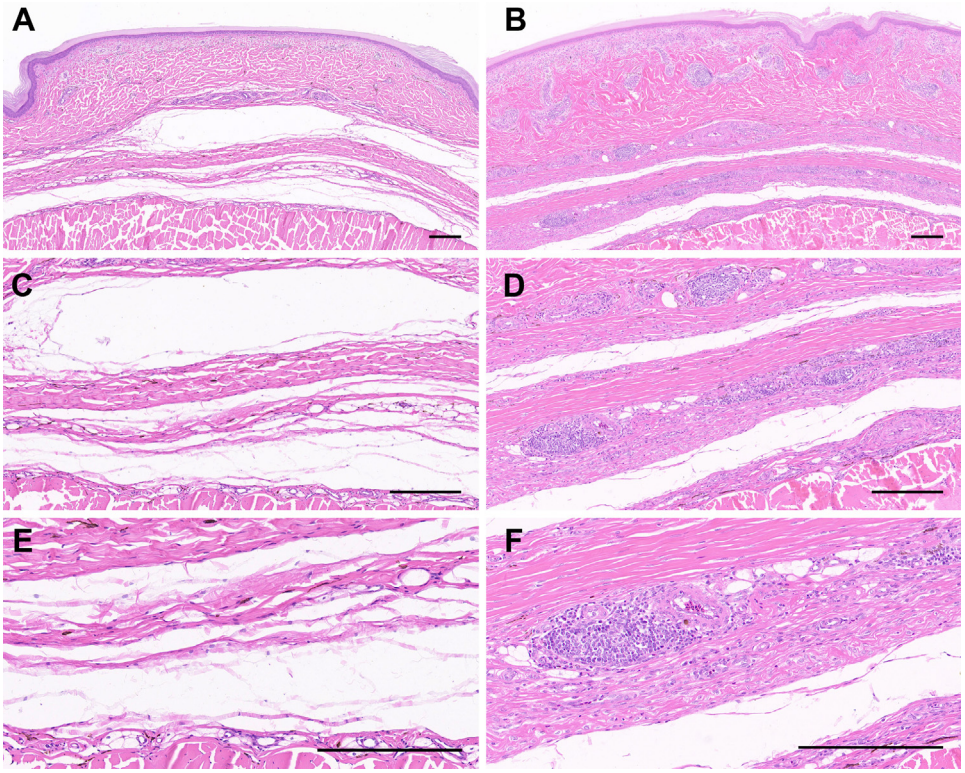

Figure 1. Pathological tissue section observation. Panels A, C, and E and panels B, D, and H show 8×, 18×, and 36× magnifications of pathological tissue sections of skin, subcutaneous tissue, tendon sheath, epitenon, and metatarsal extensor from the uninfected chickens and the chickens infected with *Mycoplasma synoviae*, respectively. The length of the bars in each figure is 200 nm.

connective tissue, the layer of synovial cells in the synovial sheath, and the epitenon outside the tendon showed proliferation of fibrous cells (Figures 1B, 1D, 1E). The layer of synovial cells in the synovial sheath showed vascular hyperplasia and extensive scattered and focal infiltration of leukocytes, including macrophages and lymphocytes (Figures 1B, 1D). The boundary between the synovial cell layer and fibrous sheath of the tendon sheath was still clear (Figures 1D, 1F). The fibrous sheath was relatively normal except the side-faced subcutaneous tissue had slight scattered leukocyte infiltration (Figure 1D). The epitenon outside the tendon showed vascular hyperplasia and scattered leukocyte infiltration around the blood vessels (Figure 1D). The metatarsal extensor tendon of the infected chicken remained normal (Figures 1B, 1D).

MS Adherence to and Invasion of SSC

As SSCs were reported to be similar to joint fibroblast-like synoviocytes, we determined the expression of the known specific surface molecular markers Cadherin-11 of joint fibroblast-like synoviocytes and CD45 of macrophage-like synoviocytes by RT-PCR to detect whether macrophages were involved in the isolated SSCs (Kohama et al., 2002; Bartok and Firestein, 2010). The HD11 cells were used as the reference for macrophages. As a result, the isolated SSCs expressed GAPDH and Cadherin-11 coding genes, but not the CD45 coding gene, whereas the HD11 cells expressed GAPDH and CD45 coding genes, but not the Cadherin-11 coding gene (Figure 2A). These results indicated that the isolated SSCs are substantially free of macrophages.

It has been reported that MG, another important avian pathogenic mycoplasma, can be stably stored in distilled water at 4°C and 22°C for 24 h (Kleven, 1985). To analyze whether it is feasible to use distilled water to lyse host cells to recover mycoplasma adhering to or invading cells, just like the method used for bacteria (Vanier et al., 2004; Si et al., 2009), we tested the viability of MS in distilled water at 25°C for 1 h. Using the method of plate counting, it was shown that MS had no significant loss under this condition (data not shown).

The colony-counting method was used to estimate the number of mycoplasma adhering to and invading cells. In adherence assays, with the MOIs increased by an order of magnitude, the numbers in the adhesion (including invasion) of MS to SSCs were significantly increased by more than 5 times (Figure 2B, $P < 0.01$). In invasion assays, there were significant increases in the MS invasion of SSCs as a function of MOI, with a 7.92-fold increase from an MOI of 0.1 to 1 and a 2.70 increase from an MOI of 1 to 10 (Figure 2C, $P < 0.01$). The average proportions of invasion with respect to the values of adherence of MS to SSC were 7.00, 10.42, and 5.35% at the MOIs of 0.1, 1, and 10, respectively.

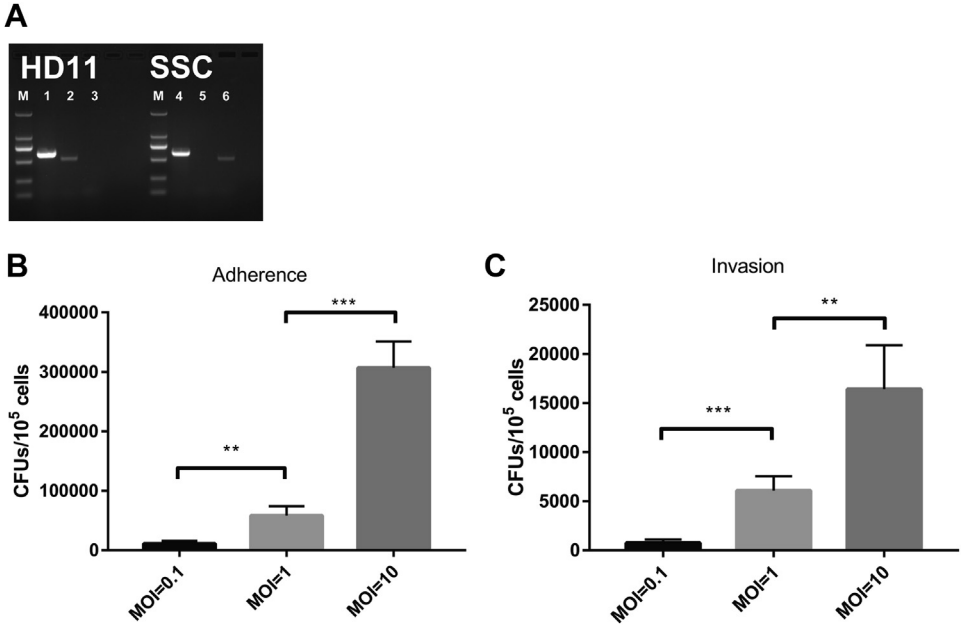

Figure 2. Identification of synovial sheath cells as well as adhesion and invasion assays. Panel A shows that the synovial sheath cells isolated in this study are substantially free of macrophages by RT-PCR assays. Lanes 1 to 3 and 4 to 6 show the expression of GAPDH, CD45, and Cadherin-11 coding genes in HD11 and synovial sheath cells (SSCs), respectively. Lane M is 2,000-bp DNA maker. Panels B and C show the numbers of CFU of *Mycoplasma synoviae* recovered from adherence or invasion of every 1×10^5 synovial sheath cells. In each group of assays, 3 different MOIs were used: ~0.1, 1, and 10. The statistical significance of the differences between every 2 samples was assessed using unpaired *t* test (**$P < 0.01$; ***$P < 0.001$).

Relative Gene Expression in SSC With Incubation of MS

To analyze the effects of MS-infected SSCs on host inflammation and immunity, we examined kinetic changes on the transcription levels of all avian Toll-like receptors (TLRs), major inflammatory cytokines, and major chemokines encoding genes in SSCs after MS infection with different MOIs at the same incubation time, or with different incubation times for the same MOI.

After 6 h of infection of SSCs with MS at an MOI of 10, the transcription levels of genes encoding IL-1β, IL-6, IL-8, CCL-20, RANTES, MIP-1β, IL-12p40, TLR7, and TLR15 in the cells increased significantly relative to the uninfected cells (Figures 3A–G and N-O, $P < 0.05$). Starting from a 6-h incubation period, the IL-1β and IL-6 genes transcription levels were constantly increasing; the RANTES and IL-12p40 gene transcription levels remained basically unchanged; the IL-8, CCl-20, MIP-1β, TLR7, and TLR15 gene transcription levels were constantly decreasing but still maintained relatively high levels within the incubation time. All coding genes mentioned previously maintained significantly high transcription levels with the 6, 12, and 24 h of incubation time relative to the uninfected cells (Figures 3A–G and N-O, $P < 0.05$).

Relative to the untreated SSCs, MS significantly increased the transcription levels of genes encoding IL-1β, IL-6, IL-8, CCL-20, RANTES, MIP-1β, TLR7, and TLR15 in SSCs after infection with SSCs for 12 h at an MOI of 0.1 (Figures 4A–F and N-O, $P < 0.05$). In addition, with both the increase of MOIs from 0.1 to 1 and 1 to 10, the transcription levels of IL-1β, IL-6, IL-8, CCL-20, RANTES, MIP-1β, TLR7, and TLR15 encoding genes were significantly increased after incubation of SSCs with MS for 12 h (Figures 4A–F and Figures 4N, 4O, $P < 0.05$). At an MOI of 0.1, MS failed to stimulate SSCs to produce significantly increased transcription levels of IL-12p40 gene during the 12-h incubation period (Figure 4G). Compared with the untreated SSCs, the transcription levels of IL-12p40 in SSCs incubated with MS at MOIs of 1 and 10 were significantly increased (Figure 4G, $P < 0.05$). Compared with stimulating cells with MS at an MOI of 0.1, stimulating cells with MS at an MOI of 10 can significantly upregulate the transcription level of IL-12p40 gene in SSCs within 12 h of incubation time (Figure 4G, $P < 0.05$).

The avian genes encoding TLR1 and TLR2 have 2 gene duplications in the genome, which are genes encoding TLR1A and TLR1B and TLR2A and TLR2B, respectively (Higuchi et al., 2008; St Paul et al., 2013). We designed primers in the homologous regions of TLR1A and TLR1B coding genes to detect the overall expression of the 2 genes and also designed primers in the nonhomologous regions of the 2 genes to detect the expression of these 2 genes. The same strategy was used to detect the TLR2A and TLR2B genes. Infecting SSCs with MS at different MOIs or at different incubation times did not significantly stimulate the cells to increase the transcription level of IFN-γ, CXCL-13, TLR1 (including TLR1, TLR1A, and TLR1B), TLR2 (including TLR2, TLR2A, and TLR2B), TLR3, TLR4, TLR5, and TLR21 encoding genes (Figures 3H–M; Figures 4H–M; Supplementary Figure 1A–F; Supplementary Figure 2A–F). Regardless of whether

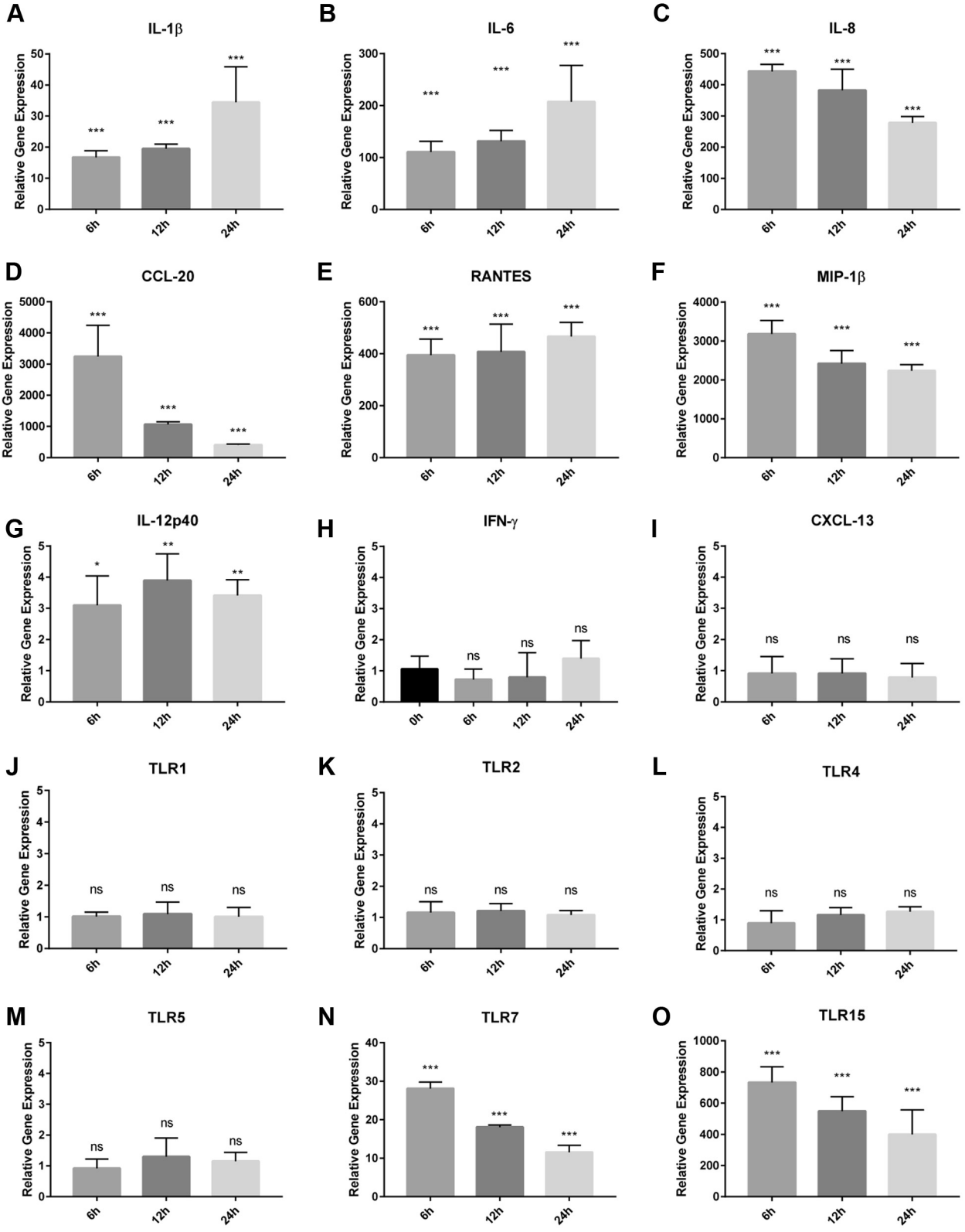

Figure 3. Relative gene expression in synovial sheath cells during inoculation with *Mycoplasma synoviae* for different times. The graphs show relative mRNA levels by qPCR of test genes (IL-1β (panel A), IL-6 (panel B), IL-8 (panel C), CCL-20 (panel D), RANTES (panel E), MIP-1β (panel F), IL-12p40 (panel G), IFN-γ (panel H), CXCL-13 (panel I), TLR1 (panel J), TLR2 (panel K), TLR4 (panel L), TLR5 (panel M), TLR7 (panel N), and TLR15 (panel O) coding genes) in synovial sheath cells incubated with *Mycoplasma synoviae* at an MOI of 10 for 6, 12, and 24 h. Data represent means and SEs of three independent experiments. The statistical significance of comparisons between synovial sheath cells incubated with *Mycoplasma synoviae* and without *Mycoplasma synoviae* for 6, 12, or 24 h was determined using unpaired *t*-test (ns, not significant; $^{*}P < 0.05$; $^{**}P < 0.01$; $^{***}P < 0.001$).

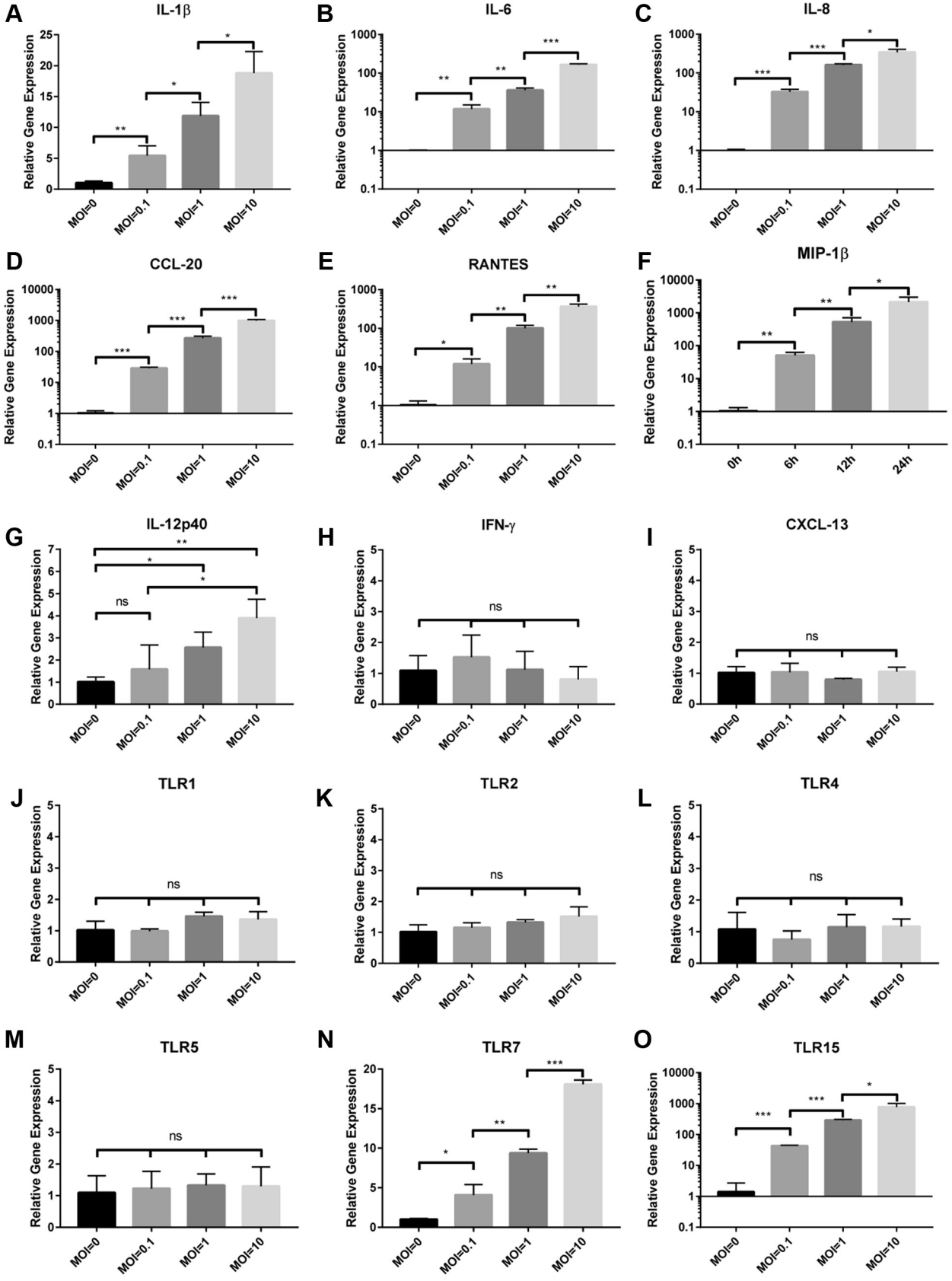

Figure 4. Relative gene expression in synovial sheath cells inoculated with different MOIs of *Mycoplasma synoviae* for 12 h. The graphs show relative mRNA levels by qPCR of test genes (IL-1β (panel A), IL-6 (panel B), IL-8 (panel C), CCL-20 (panel D), RANTES (panel E), MIP-1β (panel F), IL-12p40 (panel G), IFN-γ (panel H), CXCL-13 (panel I), TLR1 (panel J), TLR2 (panel K), TLR4 (panel L), TLR5 (panel M), TLR7 (panel N), and TLR15 (panel O) coding genes) in synovial sheath cells incubated with *Mycoplasma synoviae* at an MOI of 0.1, 1, or 10 for 12 h. Data represent means and SEs of three independent experiments. The statistical significance of comparisons between two samples was determined using unpaired *t*-test (ns, not significant; $^{*}P < 0.05$; $^{**}P < 0.01$; $^{***}P < 0.001$).

the SSCs were infected by MS, the corresponding C_T values of the TNF-α and GM-CSF could not be detected by the qPCR method. Thus, the cells cannot express these 2 genes, regardless of whether they are infected by MS.

Stimulating Effects of Secretions From MS-Infected SSCs on Macrophage Chemotaxis and Cytokine Production

In the chemotaxis assay, when macrophages were stimulated with MIP-1β, the number of migrated macrophages was significantly higher than the number of migrated macrophages stimulated with the culture medium from SSCs infected with MS at an MOI of 10 (Figure 5, $P < 0.05$). With the increase of MOIs from 0.1 to 1 as well as 1 to 10 when MS infected SSCs, the culture medium from MS-infected SSCs significantly increased the number of macrophage migration after stimulating macrophages (Figure 5, $P < 0.05$). The number of migrated macrophages after macrophages were stimulated with the culture medium from MS-infected SSCs (at an MOI of 0.1) was significantly increased relative to the culture medium from uninfected MS (Figure 5, $P < 0.05$). In addition, the transcriptional levels of some cytokine-encoding genes in HD11 cells incubated with conditioned medium from SSCs infected with MS at an MOI of 10 were tested. The results showed, relative to the HD11 cells cocultured with uninfected SSCs, that the transcription levels of IL-1β, IL-6, IL-8, CCL-20, RANTES, MIP-1β, and CXCL-13 encoding genes in HD11 cells after incubation with conditioned medium from MS-infected SSCs were significantly increased (Figure 6, $P < 0.01$). In contrast, there were no significant differences in the transcription levels of IL-12p40 and IFN-γ coding genes between the 2 kinds of treatments on HD11 cells (Figure 6, $P > 0.05$). To confirm that there were no viable MS in coculture supernatants, supernatants were cultured in modified Frey medium for up to 7 d with no evidence of growth. In addition, ELISA detection of supernatants in the MS antigen was negative (data not shown).

DISCUSSION

One of the typical pathogenic features of MS is that it can cause synovitis in chickens. However, studying the pathogenic mechanism of mycoplasma using the host cells as targets *in vitro* in previous research, the cells' species from chickens included macrophages, erythrocytes, embryonic fibroblasts, and chondrocytes, but no synovial cells (Lavric et al., 2008; Dusanic et al., 2009). Thus, the interaction between mycoplasma and synoviocytes in the development of synovitis, especially in the chemotaxis of immune cells as one of the major causes of synovial tissue lesion, was the focus of this study.

Synovial tissues cover high-friction areas where they provide lubrication for the mechanical movement of their wrapped objects, such as movable joints and tendons (Iwanaga et al., 2000; Wang et al., 2017). A synovial sheathed tendon has 3 distinct components: the tendon proper, consisting of longitudinally oriented collagen fibrils and cells, an epitenon on the tendon, which tends to be circumferentially oriented about the tendon, and a circumferentially oriented fibrous sheath associated with a synovial layer (Greenlee et al., 1975). In the case of the tendon sheath synovium, previous studies have shown that the lesions of metatarsal extensor tendons after an MS infection are more severe and typical relative to other tendons (Lockaby et al., 1998). However, the observation of the relevant

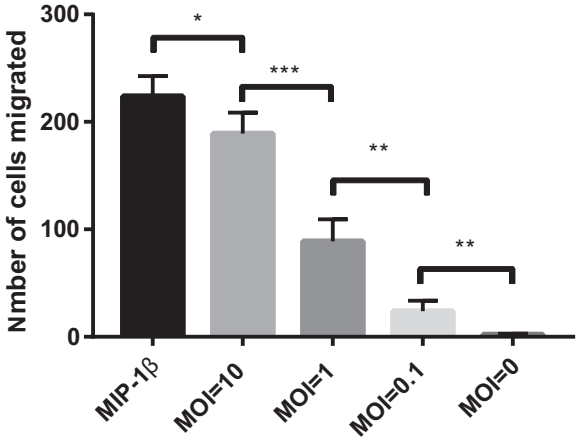

Figure 5. Chemotaxis assays. HD11 cells were assayed for chemotaxis in response to different kinds of culture supernatants of synovial sheath cells. Chicken recombinant MIP-1β mixed in the culture supernatant of uninfected synovial sheath cells was used as a positive control. The culture supernatant of uninfected synovial sheath cells served as a negative control. Data represent means and SEs of 3 independent experiments. The statistical significance of comparisons between 2 samples was determined using unpaired *t* test (*$P < 0.05$; **$P < 0.01$; ***$P < 0.001$).

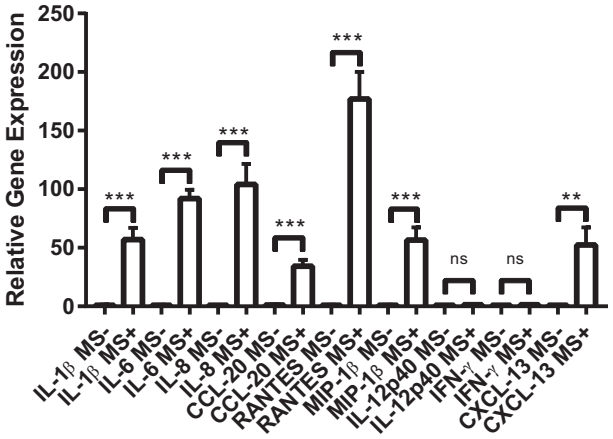

Figure 6. Relative gene expression in HD11 cells incubated with culture supernatants of *Mycoplasma synoviae*–infected synovial sheath cells. The graph shows the relative mRNA levels by qPCR of test genes in HD11 cells incubated with culture supernatant of MS infected or uninfected synovial sheath cells. Data represent means and SEs of 3 independent experiments. The statistical significance of comparisons between 2 samples was determined using unpaired *t* test (ns, not significant; **$P < 0.01$; ***$P < 0.001$).

pathological sections did not reflect well the tissue structure of the synovial sheath. Therefore, this new study was conducted. The results revealed that the infiltration of inflammatory cells is mainly concentrated on the synovial layer of tendon sheath, rather than the tendon and fibrous sheath (Figures 1B, 1D, 1F). This observation indicates that synovial cells play a major role in the process of chemotaxis of inflammatory cells that leads to the infiltration of inflammatory cells. The fibroblast-like synoviocytes in the synovial membrane of the joint are widely present in the surface layer of the synovial membrane, and the macrophage-like synoviocytes of the tendon sheath synovium are only present in the mesentery (Kohama et al., 2002; Tu et al., 2018). This indicates that the inflammatory cell infiltration of the tendon sheath synovium is mainly caused by the reaction of fibroblast-like synoviocytes in the synovium, here described as SSCs as others have done (Ozturk et al., 2008).

Bacteria and mycoplasma usually first establish a specific and firm attachment to their target cells through a process known as cytoadhesion to colonize, infect, and avoid rapid clearance by the innate host defense mechanisms. This is also a prerequisite for the initiation of the processes that result in host cell alterations and pathogenesis. For example, compared to the MG virulent R_{low} strain, the avirulent MG R_{high} strain lacks 2 cytoadhesin-relative molecules (GapA and CrmA), which significantly attenuated the cytoadherence capabilities and the colonization ability in the chicken respiratory tract, as well as the lesions in chicken tracheas and air sacs, and reduced the number and extent of multiple cytokine-encoding genes that are upregulated in stimulated chicken tracheal epithelial cells (Levisohn et al., 1986; Papazisi et al., 2000; Indikova et al., 2013; Majumder et al., 2014).

Our study found that with the increase of the MOIs, the adhesion and invasion of MS increased significantly (Figure 2), which was accompanied by a significant increase in the stimulation of the expression of various pattern-recognition receptors, inflammatory cytokines, and chemokines-coding genes, such as genes encoding IL-1β, IL-6, IL-8, CCL-20, RANTES, MIP-1β, IL-12p40, TLR7, and TLR15 in SSCs (Figure 4), and also an increase in the chemotaxis of macrophages (Figure 5). These findings indicate that the interaction of MS with SSCs contributes to macrophage recruitment and inflammation, as well as suggest that the infection number of MS to SSCs plays an important role in the development of synovitis, especially in the synovial lesion caused by inflammatory cell infiltration. In addition to the previous reports showing that MS can invade chicken erythrocytes, chondrocytes, and embryo fibroblasts (Dusanic et al., 2009), our study also demonstrated that MS can get inside SSCs (Figure 2C), which indicates that MS can invade a wide range of cells, which helps it escape identification and attack host innate immunity. As far as we know, the MS lacks known adhesion factors and homologs of adhesion factors present in other mycoplasmas, such as GapA and CrmA in MG, MgpC and P1 in *Mycoplasma pneumoniae*, and MgPa in *M. genitalium* (Papazisi et al., 2000; Burgos et al., 2006; Meng et al., 2017). The study of hemagglutinin of MS, which also exists in MG, is also limited to the agglutination of erythrocytes (May et al., 2014). Therefore, screening and identification of cell adhesion molecules important for MS require further studies.

So far, 10 kinds of TLR in chickens have been established, namely, TLR1A, TLR1B, TLR2A, TLR2B, TLR3, TLR4, TLR5, TLR7, TLR15, and TLR21 (St Paul et al., 2013; Velova et al., 2018). We examined the expression of these TLRs after MS stimulated SSCs, and the results showed that only TLR7 and TLR15 were significantly upregulated after MS stimulation of SSCs (Figures 3N, 3O and Figures 4N, 4O). TLR15 is a specific pattern-recognition receptor for avian species (Boyd et al., 2012; Oven et al., 2013). It has been reported that MS was capable of inducing TLR15 expression in chicken chondrocytes and macrophages, which led to NF-κB activation and nitric oxide production (Oven et al., 2013). We found a significantly higher expression of TLR15, but not of the other cellular outer membrane located TLRs (TLR1A, TLR1B, TLR2A, TLR2B, TLR4, and TLR5) when SSCs were simulated with MS (Figures 3 and 4, Supplementary Figures 1 and 2). These results indicate that the major pattern-recognition receptor that causes inflammatory responses to stimulation of MS by chicken-derived cells is TLR15. Besides, the expression level of TLR7 was unexpectedly found to be significantly increased in the SSCs that had been infected with MS (Figure 3N and Figure 4N). As a TLR of the main endosomal compartment localization of cells, TLR7 has been reported to mainly recognize the uridine-rich or uridine/guanosine-rich ssRNA of viral and host origins (Diebold et al., 2004; Heil et al., 2004; Keestra et al., 2013). Besides, TLR7 in macrophages infected by the intracellular bacterium *Mycobacterium tuberculosis* was significantly upregulated (Bao et al., 2017). The G + C content of the MS genome is only about 28% (Zhu et al., 2018). The transcribed RNA of MS is rich in uridine. After invading host cells, MS often enter endosomal vesicles (Walker et al., 1978). We also demonstrated that MS can invade SSCs (Figure 2C). These may be the reasons for the induction of TLR7 expression by MS-stimulated SSCs.

It has been reported that the recognition, phagocytosis, and degradation of mycoplasma by macrophages in innate immunity play a major role in controlling and eliminating mycoplasma infection (Erb and Bredt, 1979; Davis et al., 1980). IFN-γ and GM-CSF are the major cytokines that activate macrophages into cells involved in pathogen killing (Chavez-Galan et al., 2015). IFN-γ–activated macrophages significantly enhanced the killing of pathogens such as *Mycoplasma pulmonis* and *Mycobacterium leprae* (Hickman-Davis et al., 1999; Bashyam, 2007). IL-12 plays an essential role in inducing IFN-γ production by macrophages (Darwich et al., 2009), whose upregulated expression

also serves as a feature of activated microbicidal macrophages (Chavez-Galan et al., 2015). This study found that MS stimulation of SSCs significantly enhanced the expression of IL-12 (Figure 3G and Figure 4G), but not IFN-γ or GM-CSF. HD11 exposed to a culture of MS and SSCs coincubation did not significantly enhance the expression of IL-12 and IFN-γ (Figure 6). These results indicated that the activation of macrophages only through secretions produced by MS-stimulating cells is insufficient. Insufficient activation of macrophages and adhesion or even invasion of mycoplasma in SSCs led to ineffective clearance of mycoplasma, the persistence of inflammation, and leucocyte infiltration, which may be why inflammation enters the chronic phase.

By histopathological observation, we found that a major cause of MS-induced pathological changes of the tendon sheath synovium was the inflammatory cell infiltration of the synovial layer. The adhesion and invasion of MS to SSCs, the stimulation of the expression of various pattern recognition receptors, inflammatory cytokines, and chemokines-coding genes, including IL-1β, IL-6, IL-8, CCL-20, RANTES, MIP-1β, IL-12p40, TLR7, and TLR15 in SSCs, and macrophage chemotaxis positively correlated with the MOIs of MS to SSCs. The interaction between MS and SSCs can activate macrophages to some extent. This study systematically demonstrated that the interaction of MS to chicken SSCs contributes to macrophage recruitment and inflammation, which is helpful to elucidate the molecular mechanism of MS-induced synovitis in chicken.

ACKNOWLEDGMENTS

This study was supported by the National Key Research and Development Program (2017YFD0500706).

Conflict of Interest Statement: The authors declare that they have no competing interests.

SUPPLEMENTARY DATA

Supplementary data associated with this article can be found in the online version at https://doi.org/10.1016/j.psj.2020.08.003.

REFERENCES

Bao, M., Z. Yi, and Y. Fu. 2017. Activation of TLR7 inhibition of *Mycobacterium tuberculosis* survival by autophagy in RAW 264.7 macrophages. J. Cell Biochem. 118:4222–4229.

Bartok, B., and G. S. Firestein. 2010. Fibroblast-like synoviocytes: key effector cells in rheumatoid arthritis. Immunol. Rev. 233:233–255.

Bashyam, H. 2007. IFNgamma: issuing macrophages a license to kill. J. Exp. Med. 204:3.

Boyd, A. C., M. Y. Peroval, J. A. Hammond, M. D. Prickett, J. R. Young, and A. L. Smith. 2012. TLR15 is unique to avian and reptilian lineages and recognizes a yeast-derived agonist. J. Immunol. 189:4930–4938.

Burgos, R., O. Q. Pich, M. Ferrer-Navarro, J. B. Baseman, E. Querol, and J. Pinol. 2006. *Mycoplasma genitalium* P140 and P110 cytadhesins are reciprocally stabilized and required for cell adhesion and terminal-organelle development. J. Bacteriol. 188:8627–8637.

Chavez-Galan, L., M. L. Olleros, D. Vesin, and I. Garcia. 2015. Much more than M1 and M2 macrophages, there are also CD169(+) and TCR(+) macrophages. Front. Immunol. 6:263.

Darwich, L., G. Coma, R. Pena, R. Bellido, E. J. Blanco, J. A. Este, F. E. Borras, B. Clotet, L. Ruiz, A. Rosell, F. Andreo, R. M. Parkhouse, and M. Bofill. 2009. Secretion of interferon-gamma by human macrophages demonstrated at the single-cell level after costimulation with interleukin (IL)-12 plus IL-18. Immunology 126:386–393.

Davis, J. K., K. M. Delozier, D. K. Asa, F. C. Minion, and G. H. Cassell. 1980. Interactions between murine alveolar macrophages and *Mycoplasma pulmonis in vitro*. Infect. Immun. 29:590–599.

Diebold, S. S., T. Kaisho, H. Hemmi, S. Akira, and C. Reis e Sousa. 2004. Innate antiviral responses by means of TLR7-mediated recognition of single-stranded RNA. Science 303:1529–1531.

Dufour-Gesbert, F., A. Dheilly, C. Marois, and I. Kempf. 2006. Epidemiological study on *Mycoplasma synoviae* infection in layers. Vet. Microbiol. 114:148–154.

Dusanic, D., R. L. Bercic, I. Cizelj, S. Salmic, M. Narat, and D. Bencina. 2009. *Mycoplasma synoviae* invades non-phagocytic chicken cells *in vitro*. Vet. Microbiol. 138:114–119.

Erb, P., and W. Bredt. 1979. Interaction of *Mycoplasma pneumoniae* with alveolar macrophages: viability of adherent and ingested mycoplasmas. Infect. Immun. 25:11–15.

Greenlee, Jr, T.K., C. Beckham, and D. Pike. 1975. A fine structural study of the development of the chick flexor digital tendon: a model for synovial sheathed tendon healing. Am. J. Anat. 143:303–313.

Heil, F., H. Hemmi, H. Hochrein, F. Ampenberger, C. Kirschning, S. Akira, G. Lipford, H. Wagner, and S. Bauer. 2004. Species-specific recognition of single-stranded RNA via toll-like receptor 7 and 8. Science 303:1526–1529.

Hickman-Davis, J., J. Gibbs-Erwin, J. R. Lindsey, and S. Matalon. 1999. Surfactant protein A mediates mycoplasmacidal activity of alveolar macrophages by production of peroxynitrite. Proc. Natl. Acad. Sci. U. S. A. 96:4953–4958.

Higuchi, M., A. Matsuo, M. Shingai, K. Shida, A. Ishii, K. Funami, Y. Suzuki, H. Oshiumi, M. Matsumoto, and T. Seya. 2008. Combinational recognition of bacterial lipoproteins and peptidoglycan by chicken Toll-like receptor 2 subfamily. Dev. Comp. Immunol. 32:147–155.

Indikova, I., P. Much, L. Stipkovits, K. Siebert-Gulle, M. P. Szostak, R. Rosengarten, and C. Citti. 2013. Role of the GapA and CrmA cytadhesins of *Mycoplasma gallisepticum* in promoting virulence and host colonization. Infect. Immun. 81:1618–1624.

Iwanaga, T., M. Shikichi, H. Kitamura, H. Yanase, and K. Nozawa-Inoue. 2000. Morphology and functional roles of synoviocytes in the joint. Arch. Histol. Cytol. 63:17–31.

Kannus, P. 2000. Structure of the tendon connective tissue. Scand. J. Med. Sci. Sports 10:312–320.

Keestra, A. M., M. R. de Zoete, L. I. Bouwman, M. M. Vaezirad, and J. P. van Putten. 2013. Unique features of chicken Toll-like receptors. Dev. Comp. Immunol. 41:316–323.

Kleven, S. H. 1985. Stability of the F strain of *Mycoplasma gallisepticum* in various diluents at 4, 22, and 37 C. Avian Dis. 29:1266–1268.

Kohama, M., J. Nio, Y. Hashimoto, and T. Iwanaga. 2002. Cellular architecture of the synovium in the tendon sheath of horses: an immunohistochemical and scanning electron microscopic study. Jpn. J. Vet. Res. 50:125–139.

Kursa, O., A. Pakula, G. Tomczyk, S. Pasko, and A. Sawicka. 2019. Eggshell apex abnormalities caused by two different *Mycoplasma synoviae* genotypes and evaluation of eggshell anomalies by full-field optical coherence tomography. BMC Vet. Res. 15:1.

Lavric, M., D. Bencina, S. Kothlow, B. Kaspers, and M. Narat. 2007. *Mycoplasma synoviae* lipoprotein MSPB, the N-terminal part of VlhA haemagglutinin, induces secretion of nitric oxide, IL-6 and IL-1beta in chicken macrophages. Vet. Microbiol. 121:278–287.

Lavric, M., M. N. Maughan, T. W. Bliss, J. E. Dohms, D. Bencina, C.L. Keeler, Jr, and M. Narat. 2008. Gene expression modulation in chicken macrophages exposed to *Mycoplasma synoviae* or *Escherichia coli*. Vet. Microbiol. 126:111–121.

Levisohn, S., M. J. Dykstra, M. Y. Lin, and S. H. Kleven. 1986. Comparison of in vivo and in vitro methods for pathogenicity evaluation for *Mycoplasma gallisepticum* in respiratory infection. Avian Pathol. 15:233–246.

Livak, K. J., and T. D. Schmittgen. 2001. Analysis of relative gene expression data using real-time quantitative PCR and the 2(-Delta Delta C(T)) Method. Methods 25:402–408.

Lockaby, S. B., F. J. Hoerr, L. H. Lauerman, and S. H. Kleven. 1998. Pathogenicity of *Mycoplasma synoviae* in broiler chickens. Vet. Pathol. 35:178–190.

Majumder, S., and L. K. Silbart. 2016. Interaction of *Mycoplasma gallisepticum* with chicken tracheal epithelial cells contributes to macrophage chemotaxis and activation. Infect. Immun. 84:266–274.

Majumder, S., F. Zappulla, and L. K. Silbart. 2014. *Mycoplasma gallisepticum* lipid associated membrane proteins up-regulate inflammatory genes in chicken tracheal epithelial cells via TLR-2 ligation through an NF-kappaB dependent pathway. PLoS One 9:e112796.

May, M., D. W. Dunne, and D. R. Brown. 2014. A sialoreceptor binding motif in the *Mycoplasma synoviae* adhesin VlhA. PLoS One 9:e110360.

McGowin, C. L., L. Ma, D. H. Martin, and R. B. Pyles. 2009a. *Mycoplasma genitalium*-encoded MG309 activates NF-kappaB via Toll-like receptors 2 and 6 to elicit proinflammatory cytokine secretion from human genital epithelial cells. Infect. Immun. 77:1175–1181.

McGowin, C. L., V. L. Popov, and R. B. Pyles. 2009b. Intracellular *Mycoplasma genitalium* infection of human vaginal and cervical epithelial cells elicits distinct patterns of inflammatory cytokine secretion and provides a possible survival niche against macrophage-mediated killing. BMC Microbiol. 9:139.

Meng, Y. L., W. M. Wang, D. D. Lv, Q. X. An, W. H. Lu, X. Wang, and G. Tang. 2017. The effect of Platycodin D on the expression of cytoadherence proteins P1 and P30 in *Mycoplasma pneumoniae* models. Environ. Toxicol. Pharmacol. 49:188–193.

Oh, K., S. Lee, J. Seo, D. Lee, and T. Kim. 2010. Rapid serodiagnosis with the use of surface plasmon resonance imaging for the detection of antibodies against major surface protein A of *Mycoplasma synoviae* in chickens. Can. J. Vet. Res. 74:71–74.

Oven, I., K. Resman Rus, D. Dusanic, D. Bencina, C.L. Keeler, Jr, and M. Narat. 2013. Diacylated lipopeptide from *Mycoplasma synoviae* mediates TLR15 induced innate immune responses. Vet. Res. 44:99.

Ozturk, A. M., A. Yam, S. I. Chin, T. S. Heong, F. Helvacioglu, and A. Tan. 2008. Synovial cell culture and tissue engineering of a tendon synovial cell biomembrane. J. Biomed. Mater. Res. A 84:1120–1126.

Papazisi, L., K. E. Troy, T. S. Gorton, X. Liao, and S. J. Geary. 2000. Analysis of cytadherence-deficient, GapA-negative *Mycoplasma gallisepticum* strain R. Infect. Immun. 68:6643–6649.

Si, Y., F. Yuan, H. Chang, X. Liu, H. Li, K. Cai, Z. Xu, Q. Huang, W. Bei, and H. Chen. 2009. Contribution of glutamine synthetase to the virulence of *Streptococcus suis* serotype 2. Vet. Microbiol. 139:80–88.

St Paul, M., J. T. Brisbin, M. F. Abdul-Careem, and S. Sharif. 2013. Immunostimulatory properties of Toll-like receptor ligands in chickens. Vet. Immunol. Immunopathol. 152:191–199.

Sun, S. K., X. Lin, F. Chen, D. A. Wang, J. P. Lu, J. P. Qin, and T. R. Luo. 2017. Epidemiological investigation of *Mycoplasma synoviae* in native chicken breeds in China. BMC. Vet. Res. 13:115.

Tu, J., W. Hong, P. Zhang, X. Wang, H. Korner, and W. Wei. 2018. Ontology and function of fibroblast-like and macrophage-like synoviocytes: how do they talk to each other and can they be targeted for rheumatoid arthritis therapy? Front. Immunol. 9:1467.

Vanier, G., M. Segura, P. Friedl, S. Lacouture, and M. Gottschalk. 2004. Invasion of porcine brain microvascular endothelial cells by *Streptococcus suis* serotype 2. Infect. Immun. 72:1441–1449.

Velova, H., M. W. Gutowska-Ding, D. W. Burt, and M. Vinkler. 2018. Toll-like receptor evolution in birds: gene duplication, pseudogenisation and diversifying selection. Mol. Biol. Evol. 35:2170–2184.

Walker, E. R., M. H. Friedman, N. O. Olson, S. P. Sahu, and H. F. Mengoli. 1978. An ultrastructural study of avian synovium infected with an arthrotropic Mycoplasma, *Mycoplasma synoviae*. Vet. Pathol. 15:407–416.

Wang, Y., X. Zhang, H. Huang, Y. Xia, Y. Yao, A. F. Mak, P. S. Yung, K. M. Chan, L. Wang, C. Zhang, Y. Huang, and K. K. Mak. 2017. Osteocalcin expressing cells from tendon sheaths in mice contribute to tendon repair by activating Hedgehog signaling. Elife 6.

Xue, J., M. Y. Xu, Z. J. Ma, J. Zhao, N. Jin, and G. Z. Zhang. 2017. Serological investigation of *Mycoplasma synoviae* infection in China from 2010 to 2015. Poult. Sci. 96:3109–3112.

Yu, Y., M. Liu, L. Hua, M. Qiu, W. Zhang, Y. Wei, Y. Gan, Z. Feng, G. Shao, and Q. Xiong. 2018. Fructose-1,6-bisphosphate aldolase encoded by a core gene of *Mycoplasma hyopneumoniae* contributes to host cell adhesion. Vet. Res. 49:114.

Zhu, L., M. A. Shahid, J. Markham, G. F. Browning, A. H. Noormohammadi, and M. S. Marenda. 2018. Genome analysis of *Mycoplasma synoviae* strain MS-H, the most common *M. synoviae* strain with a worldwide distribution. BMC Genomics 19:117.